Journal of Colloid and Interface Science **244,** 211–219 (2001)
doi:10.1006/jcis.2001.7996, available online at http://www.idealibrary.com on IDEAL®

LETTER TO THE EDITOR

Citrate Enhanced Uranyl Adsorption on Goethite: An EXAFS Analysis

Citric acid promotes the adsorption of uranyl (U(VI) as UO_2^{2+}) on goethite (α-FeOOH) at pH $\leq$ 5. Enhanced adsorption does not appear to follow a simple stoichiometric relationship between total citrate and total uranyl. An excess of citric acid relative to uranyl, or a high concentration of surface-bound citrate is required. An extended X-ray absorption fine structure spectroscopy (EXAFS) study was conducted to help understand the surface interactions between citrate, UO_2^{2+}, and goethite between pH 3.5 and pH 5.5. Two principal surface species were found to be necessary and sufficient to describe the uranyl EXAFS spectra for the range of adsorbed citrate concentrations studied. (The possibility of additional minor surface species has not been eliminated, but inherent uncertainties in the data do not permit their clear identification.) One species is identified as an inner-sphere, uranyl–goethite complex, which exists at pH 5.5 in the absence of citrate. A second species is interpreted to be an adsorbed uranyl + citrate complex, which displaces the binary uranyl–goethite complex as the concentration of adsorbed citrate increases. The EXAFS spectra from samples with intermediate adsorbed citrate concentrations were reproduced using linear combinations of the spectra from these two end-member species. The uranyl + citrate surface complex appears to dominate adsorbed uranyl speciation at ligand : metal ratios of 10 : 1, or when the total surface-bound citrate approaches saturation. Although the exact structural configuration for the uranyl + citrate surface complex cannot be identified at this time, coordination between uranyl and one or more citrate molecules appears to involve both a bidentate bond (four-membered ring structure) and a putative eight-membered ring structure. The distribution and type of surface species should provide useful constraints on the development of model simulations of surface complexation behavior in this system.

Key Words: **surface complexation; adsorption; uranyl; uranium; U(VI); citrate; citric acid; tricarballylic acid; acetate; acetic acid; EXAFS; X-ray absorption spectroscopy; organic ligand.**

INTRODUCTION AND BACKGROUND

Adsorption models that simulate partitioning of solutes on mineral surfaces range from those that are highly empirical and system-specific to more mechanistic approaches that incorporate molecular level interactions and stoichiometric relationships. Surface complexation models (SCMs) are representative of the latter (see Ref. 1). Although SCMs are difficult to apply in complex natural systems they are nevertheless important for interpreting general correlations between macroscopic solute partitioning and thermodynamic relationships between individual system components. Fundamental to the development and possible application of these adsorption models is the ability to identify the types and relative proportions of surface complexes in experimental systems and to search for consistency between reaction stoichiometry and the structure of chemical species.

In this study, we are interested in the interactions between organic ligands and heavy metals at mineral oxide surfaces. The structures of ternary adsorption complexes (defined herein to involve metal ions, anionic complexing ligands, and metal oxide surfaces) are not well characterized. Our specific model system contains citric acid (2-hydroxy-1,2,3-propanetricarboxylic acid), goethite (α-FeOOH), and U(VI) as the uranyl ion, UO_2^{2+}. Citrate and goethite are representative of common constituents of soil and groundwater systems (e.g., (2, 3)). Uranyl is a high-priority contaminant at many DOE sites.

In the absence of complexing ligands, uranyl adsorption on goethite increases from nearly zero below pH 3.5 to approximately 95% above pH 5 (4).[3] In the experimental systems, uranyl adsorption was not significantly affected by citrate as long as its concentration was less than a factor of 2 greater than uranyl, and the surface concentration of citrate was well below the surface capacity. However, at higher citrate concentrations (20–100 μM citrate, 1 μM UO_2^{2+}), adsorption of uranyl between pH 3 and pH 5 increases up to ~95%. Under these conditions the surface citrate concentration is equivalent to 0.2–0.8 molecules nm^{-2} (possibly approaching monolayer coverage depending on the orientation of citrate on the surface). Model-based interpretations of traditional macroscopic measurements often cannot provide distinguishing stoichiometric signatures for the surface reactions. Deducing speciation from adsorption as a function of pH is model dependent as a consequence of different approaches used to account for the influence of electrostatic surface potential on the free energy of surface complexes.

EXAFS spectroscopy was used to characterize the local coordination environment of uranyl adsorbed on goethite in the presence of citrate under aqueous conditions. Of particular interest was the distribution of uranyl species under the conditions where uranyl is strongly sorbed with or without citrate (e.g., at or above pH 5.5 where uranyl adsorption remains >95%). In anticipation of possible types of metal ligand coordination that could be present, two additional ligands were included in the test samples. The –OH deficient citrate analog, tricarballylic acid (1,2,3-propanetricarboxylic acid), which was also found to promote the adsorption of uranyl on goethite under similar conditions, was used to help understand the significance of the hydroxyl group of citrate in the interaction between citrate and adsorbed uranyl. Aqueous uranyl–acetate complexes were included as structural models for bidentate four-membered –U–O–C–O– rings (5).

METHODS

Reagents used were uranyl nitrate hexahydrate (Johnson Matthey), trisodium citrate dihydrate (Mallinckrodt, Reagent Grade), tricarballylic acid (Aldrich, 1,2,3-propanetricarboxylic acid), anhydrous sodium acetate (Sigma), $Fe(NO_3)_3 \cdot 9H_2O$ (Baker, Analyzed Reagent), NaOH (Baker, CO_2-free), and HCl (Baker, Conc. Reagent). Water was deionized to ~18 MΩ. Goethite was

[3] Experimental conditions: 1 μM UO_2^{2+}, 68 m^2 L^{-1} goethite, 0.1 M NaCl, $P_{CO_2} \sim 0$.

0021-9797/01 $35.00

TABLE 1
EXAFS Sample Parameters

Sample	pH	T_{Ligand} (mM)	T_U (mM)	Goethite (g/L)	Γ_U[a] (μmol/m^2)
$(UO_2)_2(Cit)_2^{2-}$(aq)	5.0	50	50	—	—
UO_2^{2+}(aq)	5.5	—	50	—	—
$UO_2(Ac)_x^{2-x}$(aq)[b]	5.5	500	10	—	—
$T_{Cit} : T_U = 10 : 1$	3.5	0.4	0.04	2	0.29
$T_{Cit} : T_U = 0$	5.5	—	.96	10	0.50
$T_{Cit} : T_U = 1 : 2$	5.5	0.02	0.04	2	0.29
$T_{Cit} : T_U = 2 : 1$	5.5	0.35	0.175	10	0.25
$T_{Cit} : T_U = 5 : 1$	5.5	0.2	0.04	2	0.29
$T_{Cit} : T_U = 10 : 1$	5.5	0.4	0.04	2	0.29
$T_{Cit} : T_U = 1.1 : 1$	3.5	0.15	0.16	4.6	0.59
$T_{Cit} : T_U = 10 : 1$	5.5	0.4	0.04	2	0.29

Note. Cit, Citric acid; Ac, acetate; T_C, tricarballylate; T_{Cit}, total citrate, mol L^{-1}; T_U, total uranyl, mol L^{-1}; NaCl, 0.1 M.

[a] This represents the maximum amount that could have been adsorbed, but not a measured amount. BET surface area for goethite samples = 70 or 56 m^2/g.

[b] Species distribution estimated to be 90% $x = 3$, 10% $x = 2$.

prepared under CO_2-free conditions in a manner similar to that described in Ref. (6). The goethite was sterilized by autoclaving prior to use, and solutions were sterilized by filtration at 0.2 μm.[4] Stirred goethite suspensions (2–10 g/L) at pH 4.5, room temperature, and 0.1 M NaCl were purged with N_2 to remove carbonate. Adjustments to the pH were made using HCl or CO_2-free NaOH. Citrate or tricarballylate, then uranyl, were added to goethite suspensions as aliquots of stock solutions. After ~8 h the suspensions were analyzed for pH and centrifuged at approx. 1700 rcf for 30 min. Since there was no noticeable change in adsorption between 4 and 8 h, 8 h was taken as adequate for a stable adsorbed concentration (shorter time periods were not studied in detail). EXAFS measurements for samples equilibrated for 8 and 48 h were essentially identical. Supernatant samples taken for dissolved iron analysis were filtered through 0.2 μm filters and acidified prior to analysis by graphite furnace automic absorption spectroscopy.

Thermodynamic speciation calculations (for 25°C) were made using the program HYDRAQL (7) with a thermodynamic database using constants obtained from Refs. (8–11). Goethite pastes were transferred under a nitrogen atmosphere to 2-mn-thick Teflon sample holders and sealed with Mylar tape. EXAFS analysis of the samples began within 12 h of sample preparation. Solution samples were loaded into 3-mm-thick Teflon sample holders or polystyrene bottles with Mylar windows. Sample conditions are summarized in Table 1. Uranium L_{III}-edge EXAFS spectra were measured at room temperature at the Stanford Synchrotron Radiation Laboratory beam-line 4-1 as described elsewhere (12) and were processed using the EXAFSPAK software (13). EXAFS spectra were obtained by subtracting a spline fit from each background-subtracted spectrum and were k^3-weighted. The EXAFS spectrum for each sample was fit with a linear combination of end-member spectra from: (a) the $T_{Cit} : T_U = 10 : 1$ sample[5] at pH 3.5 and (b) the pH 5.5 citrate-free samples using nonlinear least squares optimization. Uncertainty in the linear combination fits was estimated by fitting a series of spectra from binary physical mixtures of model compounds (autunite/schoepite and autunite/adsorbed uranyl) (14). These solids were chosen because they could be measured out as single components and because their EXAFS contain the general types of spectral features observed in these systems. Nonsystematic error was found to be dominated by the spline function used to isolate the EXAFS, leading to ca. 6% deviation, 1σ. Systematic error up to 6% was observed and attributed to slight differences in normalization values for different model compounds. Principal component analysis (single value decomposition) of selected spectra was conducted using the program WinXAS (15), following the theory and procedures outlined by Wasserman (16) and Ressler (17).

Samples with conditions that favored end-member speciation (i.e., uranyl + citrate + goethite at pH 3.5 and uranyl + goethite at pH 5.5) were analyzed using shell-by-shell simulations of the spectra based on phase and amplitude functions obtained from FEFF 7 (18, 19). To improve the sensitivity toward fitting shells beyond the nearest neighbor oxygens, the fitted U–O_{axial} and U–$O_{equatorial}$ components were subtracted from the EXAFS spectra to produce residual EXAFS spectra, which were subsequently fit. In no instance did the number degrees of freedom during fitting exceed the total number allowed to vary, N_{free}, according to $N_{free} = 2(\Delta k)(\Delta R)/\pi$, where Δk is the range of k space being fit, and ΔR is the width of the characteristic frequency in the Fourier Transform (FT). For the pH 3.5 and 5.5 citrate/carballylate + uranyl sorption samples, it was necessary to constrain the Debye-Waller (σ^2) values for carbon to prevent them from floating to unrealistically low values (i.e., <0.001 Å^2). We speculate that this tendency is related to the use of harmonic σ^2 terms in a system (i.e., ring structures) where asymmetric distributions of U–C distances are likely to occur, which can lead to underestimation of σ^2 and/or CN (20). In the present case, the data ranges do not allow additional degrees of freedom required for anharmonic fits, nor is it justified to use any given anharmonic model. Calculations on multiple scattering (MS) in the uranyl cation were performed using the four-legged path, U=O_{axial}=U=O'_{axial}=U, based on its ability to fit model compound spectra and on previous investigations regarding this multiple scattering path in U L_{III}-edge EXAFS (12, 21). Accuracies of bond distances and coordination numbers (CNs), relative to XRD structure reports, were estimated to be ±0.03 Å and ±30%, respectively (12, 22).

The potential for formation of precipitates or dissolution of goethite by citrate are worth noting. Dissolution of goethite should not interfere with the conclusions of this study if the product is simply dissolved iron species and there is not significant sequestration of citrate. Thermodynamic calculations predict that significant dissolution of goethite could occur due to the formation of $FeOHCit^-$(aq) at pH below 4.5. However, an analysis of total iron by atomic absorption has shown dissolved $Fe_{total} < 0.1$ μM for the sorption samples. The rate of dissolution appears to be slow relative to the time scale of the experiments. Furthermore, thermodynamic predictions do not yet include citrate–goethite surface complexes, which will moderate the formation of dissolved Fe–citrate species. Formation of an adsorbed iron–citrate species is also a possibility. However, FTIR analysis of this system (G. D. Redden and P. Persson, 1999, unpublished data) does not indicate the presence of a surface complex between adsorbed citrate and dissolved iron within the experimental timeframe. Formation of a uranyl–citrate precipitate in the presence of goethite was also a concern. However, this possibility was discounted because solution samples prepared with uranyl and citrate concentrations higher than those in equilibrium with adsorbed uranyl and citrate showed no evidence of precipitation.

RESULTS AND DISCUSSION

EXAFS spectra for uranyl adsorbed on goethite in the presence of citrate at pH 3.5 and 5.5 are shown in Fig. 1. Spectra for model species (UO_2^{2+}(aq), $(UO_2)_x(citrate)_x^{x-}$-(aq), $UO_2(acetate)_x^{2-x}$(aq)), and uranyl adsorbed in the absence of citrate are also shown. Species distributions for the solution samples were calculated for the conditions listed in Table 1. The solution containing uranyl and citrate is predicted to be composed of approximately 90% of the $(UO_2)_2(citrate)_2^{2-}$(aq) complex and 10% of the $UO_2(citrate)^-$(aq) complex.[6]

[4] Autoclaving goethite and filter-sterilizing solutions were found to be necessary and effective to prevent biodegradation of citrate. Autoclaving goethite had no obvious effect on the surface titrations or the XRD spectrum for the material.

[5] The $T_{Cit} : T_U$ nomenclature refers to the ratio of total citrate to total uranyl in a system.

[6] Note: A recent determination of the uranyl–citrate stability constants by Borkowski *et al.* (23) apparently did not consider the formation of a 2 : 2 complex in their analysis. Other spectroscopic studies (24, 25) indicate that this species probably exists and can be significant. Therefore, formation constants from Rajan and Martell (8) were used in the calculations.

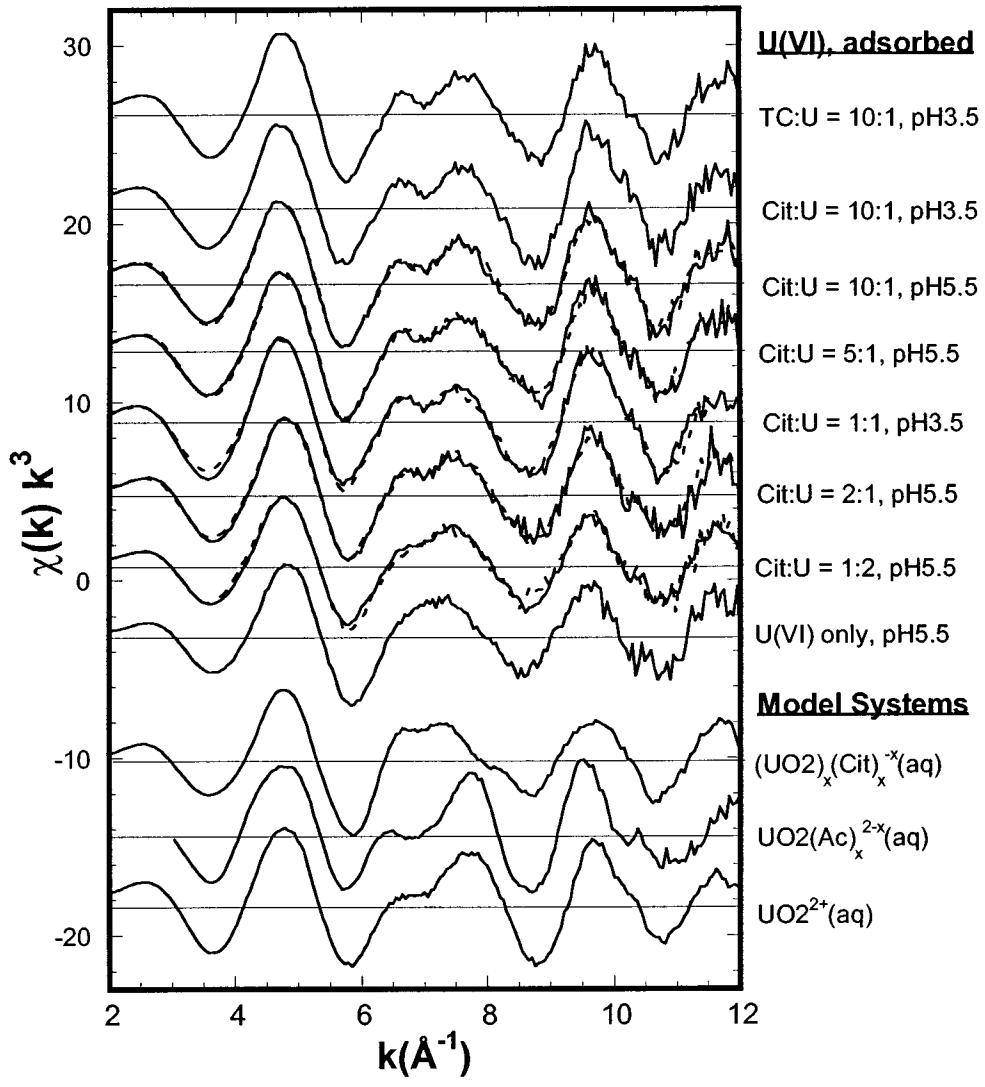

FIG. 1. EXAFS spectra for model uranyl systems and uranyl adsorbed on goethite in the presence of citric acid. Dashed lines are best-fit linear combinations (see Table 2) of spectra from the binary (uranyl only, pH 5.5) and proposed ternary ($T_{Cit} : T_U = 10 : 1$, pH 3.5) complexes. The pH of the three model systems was 5.5 (Cit, citrate; Ac, acetate; Tc, tricarballylate).

The uranyl–acetate solution complex, used as a model for a bidentate structure (four-membered U–O–C–O ring resulting from uranyl coordination with the carboxyl group) is predicted to be a mix of <1% $UO_2(acetate)^+(aq)$, 9% $UO_2(acetate)_2^0(aq)$, and 91% $UO_2(acetate)_3^-(aq)$ species at pH 5.5.

From an initial inspection of the extracted EXAFS spectra shown in Fig. 1, four qualitative conclusions can be drawn.

(i) The uranyl + citrate + goethite[7] spectra are clearly different from that of $(UO_2)_2(citrate)_2^{2-}(aq)$. Therefore, the adsorbed uranyl species are structurally distinct from the uranyl–citrate solution species.

(ii) Although uranyl + citrate + goethite spectra bear some resemblance to the spectra for $UO_2^{2+}(aq)$, and $UO_2(acetate)_x^{2-x}(aq)$, differences are apparent in the $k = 6$ to 11 A^{-1} region. These differences are more apparent in the residual spectra when the strong $U–O_{axial}$ and $U–O_{equatorial}$ components are subtracted from the total EXAFS spectra (Fig. 2).

(iii) Spectra for the samples with $T_{Cit} : T_U = 10 : 1$ at pH 3.5 and 5.5 are similar to one another. This suggests that the dominant uranyl species, or mix of species, is the same in both cases. Spectra for these two samples are also different from the spectrum for uranyl adsorption at pH 5.5 without citrate. Since uranyl does not adsorb significantly onto goethite at pH 3.5 and in the absence of citrate (4), this emphasizes the association between uranyl and citrate in both samples.

(iv) As the $T_{Cit} : T_U$ ratio decreases the spectra appear to progress toward the spectrum for uranyl adsorbed to goethite in the absence of citrate.

To test the proposal that two principal surface species can be used to describe adsorbed uranyl in the presence of citrate, the set of spectra were fit with a simple linear combination of the pH 3.5, $T_{Cit} : T_U = 10 : 1$, spectrum plus the spectrum for the uranyl + goethite sample at pH 5.5 (no citrate). As shown by the dashed lines in Fig. 1, all major features of the spectra could be reproduced in this way. The relative contributions of each of the end-member component spectra in the linear combinations are summarized in Table 2. Adding spectra for any of the three aqueous species in the analysis did not improve these fits. Likewise, substituting the spectrum for pH 3.5, $T_{Cit} : T_U = 10 : 1$ with any of the aqueous species could not reproduce the linear combination behavior.

[7] The notation "$x + y + z$" is used to indicate samples with the indicated combination of constituents.

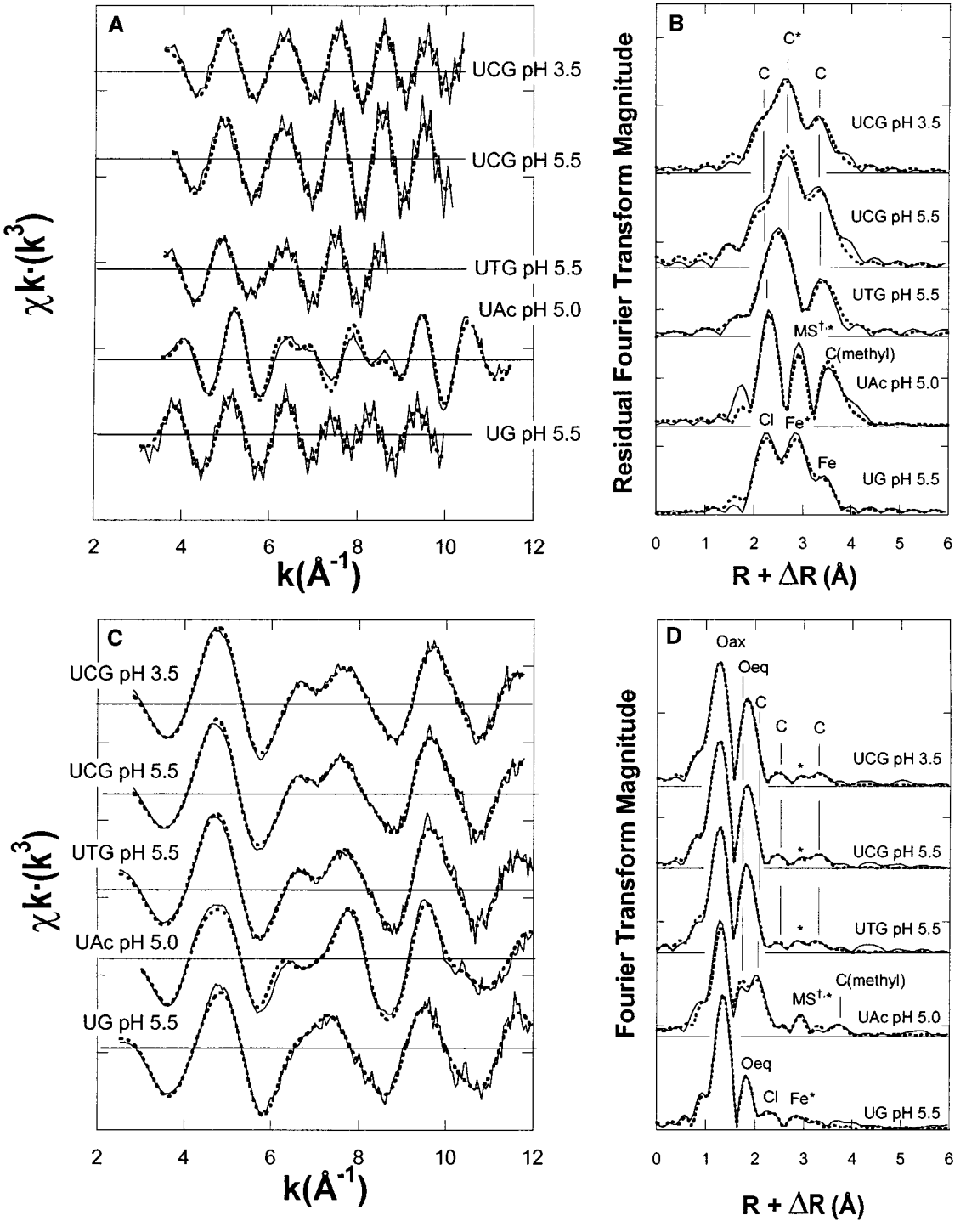

FIG. 2. (A) Residual EXAFS spectra generated by subtraction of O_{axial} and $O_{equatorial}$ shells. (B) Fourier transform (FT) plots for EXAFS residual spectra. (C) Total EXAFS spectra. (D) FT plots for total EXAFS data. Solid lines are experimental data. Dashed lines are fit results based on parameter optimization. U, uranyl; C, citrate; T, tricarballylate; Ac, acetate; G, goethite. UCG/UTG samples have ligand : U = 10 : 1. *This feature also contains the U = OMS frequency. †Triangular U–$C_{carboxy}$–O_{eq}–U MS frequency. See text for details.

TABLE 2
Two Component, Least-Squares Fits to Sample Spectra

Sample	pH	Fitting components %A	%B
$T_{Cit} : T_U = 10 : 1$	3.5	100[a]	0[a]
$T_{Cit} : T_U = 0 : 1$	5.5	0	100
$T_{Cit} : T_U = 1 : 2$	5.5	46.2	53.8
$T_{Cit} : T_U = 2 : 1$	5.5	58.6	41.4
$T_{Cit} : T_U = 1 : 1$	3.5	68.0	32.0
$T_{Cit} : T_U = 5 : 1$	5.5	87.3	12.4
$T_{Cit} : T_U = 10 : 1$	5.5	100.0	0.0

Note. Component "A": pH 3.5, $T_{Cit} : T_U = 10 : 1$; and Component "B": pH 5.5, uranyl only, no citrate. Uncertainty is estimated at 6% (1σ) from study of binary physical mixtures of model compounds. See text for details. Fit derived standard deviations fall well below this level and hence are not quoted.

[a] Consideration of component "B" did not improve the spectrum simulation, but cannot be discounted.

This system was also analyzed by single value decomposition (principal component analysis) using WinXAS, following the theory and procedures outlined previously by Wasserman (16) and Ressler (17). All uranyl + citrate spectra that had been previously fitted with linear combinations of the pH 3.5 and pH 5.5 end members were used to construct the $\boldsymbol{A}$ matrix, which was decomposed (by WinXAS) according to $[\boldsymbol{A}] = [\boldsymbol{E}] \times [\boldsymbol{V}] \times [\boldsymbol{W}]^T$, where $[\boldsymbol{E}]$ contains the eigenvectors describing an orthogonal basis set spanning the space defined by the spectra, $[\boldsymbol{V}]$ is the eigenvalue matrix, and $[\boldsymbol{W}]^T$ is the transpose of an $n \times n$ orthogonal matrix. This procedure was conducted using multiple permutations of spline fits (i.e., number of spline ranges, spline weighting) to spectra in order to assess the uncertainty arising from spline misfit. Two eigenvectors (i.e., components) were required to account for all major features in the spectra. Addition of a third component to the basis set yielded minor improvements to the reconstructed spectra (cf., Fig. 3). The sum of residuals (i.e., the differences between original and reconstructed spectra) obtained with three components was 22% smaller on average than with two components. The amount of residual and the locations (in E or k space) of poor spectral reproduction varied depending upon the choice of spline. Hence, a substantial fraction of the residual decrease associated with the third component could be attributed to uncertainty in the spline fit. The third and higher components also contribute high-frequency noise

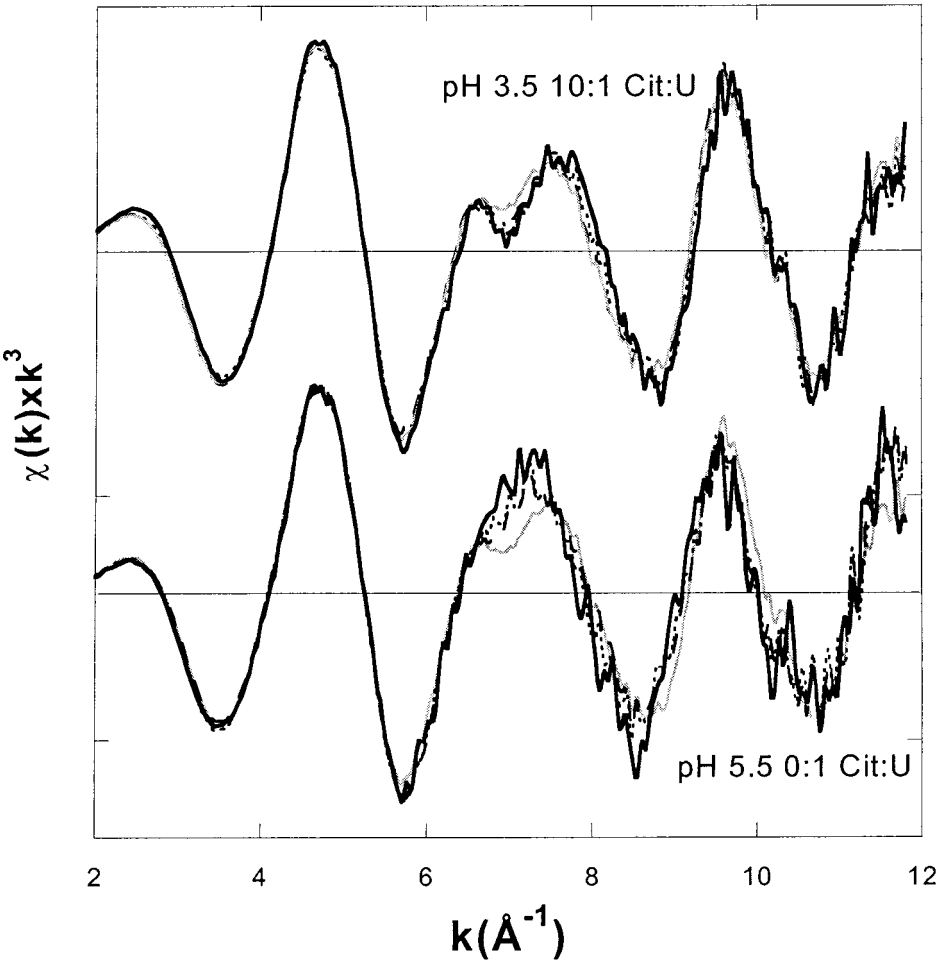

FIG. 3. Target transformation results for the pH 3.5 10 : 1 and pH 5.5 no-citrate samples. Solid black lines show the experimental data. Transformed spectra are given by the gray lines (one-component basis set), black dashed lines (two-component basis sets), and black dotted lines (three-component bases).

(derived from the original spectra) to reconstructed spectra, which can lower the sum of residuals by 10 to 20%. These observations and the excellent fits obtained with two components (Fig. 1) suggest the spectra to be dominated by two components. However, the presence of a third minor component cannot be eliminated.

The pH 3.5 $T_{Cit} : T_U = 10 : 1$ and pH 5.5 $T_{Cit} : T_U = 0 : 1$ spectra were tested for their suitability as end-member components using the target transform procedure, which projects vectors onto the space spanned by [$\boldsymbol{E}$]. This procedure will distort the spectra if they are not consistent with the data. The target transformed and original spectra are compared in Fig. 3. The one-component transforms resemble the average of the spectra and are different from the original spectra. The two-component target transformed spectra closely resemble the original spectra, suggesting they are plausible end-member components. Only minor improvements in the transformed spectra are obtained when three components are used, and, as discussed above, the improvement may be partially attributed to uncertainty caused by the spline fits.

In subsequent discussions regarding Fourier transforms (FTs), all peak distances reported are uncorrected for phase shift (i.e., $R + \Delta R$). However, we refer to true interatomic distances in all discussions regarding quantitative fit results and hypothetical structures.

Structural information about uranyl adsorbed to goethite in the absence of citrate was obtained from shell-by-shell theoretical fits to the pH 5.5 uranyl + goethite sample EXAFS. Fit results, summarized in Table 3, confirm the known transdioxo structure (U–O distance for linear O=U=O $\approx$ 1.77 to 1.79 Å) in this and the other samples. Fitting the uranyl + goethite spectrum also yields backscattering neighbors at 3.36 Å and 4.16 Å, which can be fit well with shells of Fe atoms. These distances are consistent with uranyl coordination to goethite surfaces via two equatorial oxygen atoms (12). Chlorine neighbors at 2.85 Å were required to fit the frequency corresponding to the Fourier transform peak at 2.3 Å (Fig. 2B), presumably as ternary ligands attached to adsorbed uranyl. We conclude that uranyl is present as an inner-sphere UO_2–goethite surface complex. In the discussion that follows, we note that this binary species coexists with a uranyl + citrate surface complex. Whether this species remains a simple binary complex in the presence of citrate, or includes citrate associated through an electrostatic interaction (or both) cannot be determined in this analysis. It is possible that the spectra for both types of species would be similar. Perturbations in the water–oxygen shell around adsorbed uranyl caused by an outer-sphere citrate bond could be minor and would result in weak or undetectable contributions to the EXAFS spectra.

The surface complex (or set of complexes) that predominates at $T_{Cit} : T_U = 10 : 1$ presumably involves an association (bonding) or interaction (e.g., stabilization through charge screening) between uranyl and citrate. Possibilities regarding the atomic arrangements between adsorbed uranyl and citrate include the following: (i) Uranyl acts as a bridging link between the goethite surface and citrate. In this case, an iron neighbor should be apparent in the EXAFS spectra (e.g., Ref. 12). (ii) A uranyl precipitate or multimer may form. The role that citrate would play in this case is not immediately obvious although the structure for the $(UO_2)_2(citrate)_2(aq)$ species elucidated by NMR (25) and EXAFS (24) shows uranium atoms held in close proximity by bridging oxygens donated by citrate. A signature of this type of surface species would be the presence of uranium backscattering in the EXAFS. (iii) Citrate can act as a bridge between goethite and uranyl. This type of complex is intuitively appealing given the multiplicity of acidic functional groups on citrate, and the fact that citrate is strongly adsorbed to goethite in the lower pH region in this study. (iv) Uranyl–citrate aqueous complexes could adsorb as outer-sphere or diffuse layer species. This possibility seems unlikely due to the negative surface charge present under the experimental conditions, and because existing thermodynamic data predicts uranyl-citrate solution complexes to be anionic. Signatures of the latter two types of complexes would be oxygen and carbon shells reflecting carboxyl and hydroxyl group coordination with uranyl, and the absence of Fe or U neighbors.

Shell-by-shell fits were performed on the "end-member" spectra for uranyl adsorbed to goethite in the presence of citrate (pH 3.5, 5.5, $T_{Cit} : T_U = 10 : 1$). Because of the complexity of the spectra, a systematic approach was followed in which fits to the residual spectra were attempted using all reasonable combinations of C, Fe, U, and Cl neighbors. Fits using Fe and U were found to provide poor descriptions of the spectra, unless the transdioxo multiple scattering feature was completely neglected. This feature has previously been discussed at length and shown to have significant amplitude, e.g., Refs. (21), (12), and FEFF 7 calculations demonstrate that there is no justification for arbitrarily neglecting this

TABLE 3
Shell-by-Shell EXAFS Fit Results

pH	$T_{ligand} : T_U$		O_{ax}	O_{eq1}	O_{eq2}	C_1 or Cl	C_2 or Fe	C_3 or Fe
3.5	Citrate	CN[a]	2.0[c]	3.9 (2)	—	C_1: 1.7 (4)	C_2: 1.8 (4)	C_3: 1.3 (4)
	10 : 1	R (Å)[b]	1.770 (1)	2.387 (3)	—	2.93 (1)	3.10 (1)	4.08 (1)
		σ^2 (Å^2)	.0032 (1)	.0060 (5)	—	0.002[d] (2)	0.002[d] (2)	0.002[d] (2)
5.5	Citrate	CN[a]	2.0[c]	3.9 (4)	—	C_1: 1.8 (6)	C_2: 1.9 (7)	C_3: 2.3 (9)
	10 : 1	R (Å)[b]	1.776 (2)	2.386 (4)	—	2.93 (1)	3.10 (2)	4.11 (1)
		σ^2 (Å^2)	.0031 (1)	.0065 (7)	—	0.004[d] (2)	0.004[d] (2)	0.004[d] (2)
5.5	No	CN[a]	2.0[c]	2.1 (5)	4.0 (5)	Cl: 0.4 (1)	Fe: 1.0 (9)	Fe: 0.3 (1)
	ligand	R (Å)[b]	1.792 (2)	2.30 (3)	2.44 (2)	2.95 (1)	3.36 (3)	4.16 (3)
		σ^2 (Å^2)	.0021 (1)	.011 (4)	.011 (4)	0.006[c]	0.016 (9)	0.010[c]
5.0	Tricarb.	CN[a]	2.0[a]	3.7 (3)	—	C_1: 2.3 (3)	C_2: 2.6 (4)	C_3: 1.9 (4)
	10 : 1	R (Å)[b]	1.770 (2)	2.391 (3)	—	2.92 (1)	3.11 (1)	4.09 (1)
		σ^2 (Å^2)	.0029 (1)	.0052 (6)	—	0.004[c]	0.004[c]	0.004[c]
5.5	Acetate	CN[a]	2.0[a]	6.0[c] (4)	—	C_1: 2.3 (2)	—	C_3: 2.3 (2)
	50 : 1	R (Å)[b]	1.772 (1)	2.439 (3)	—	2.843 (3)	—	4.293 (4)
		σ^2 (Å^2)	.0021 (1)	.0084 (5)	—	.0040 (5)	—	0.007 (1)

[a] Coordination number (±30%).
[b] Interatomic distance (±0.03 Å).
[c] Parameter value held constant.
[d] Parameter values linked during fits. Estimated standard deviations are given in parentheses and refer to the last digit of the numerical result. The 99.5% confidence interval limits are obtained by multiplying the ESDs by 2.81 (eq, equatorial).

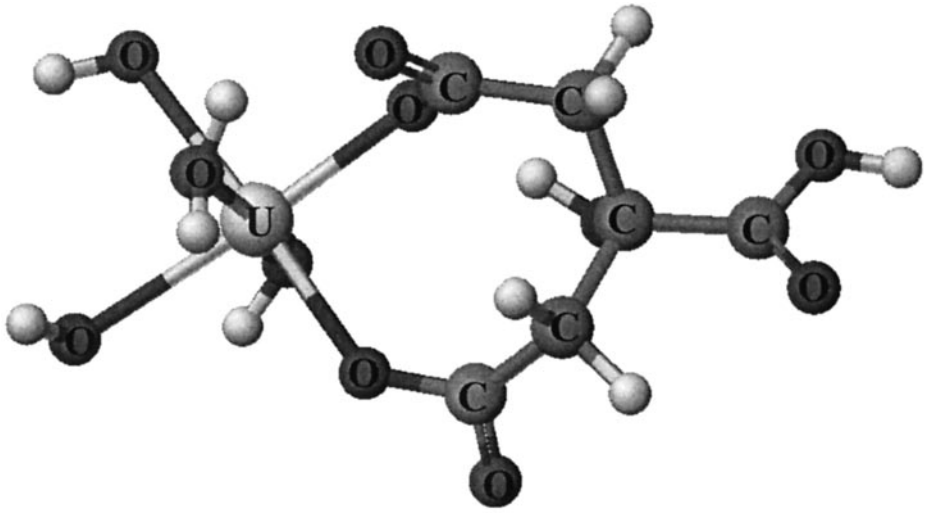

FIG. 4. Molecular structure of eight-membered ring Cd(II)$(OH_2)(H_2O)_2$–citrate complex calculated using the PM3 Hamiltonian. See text for details.

feature (12). The absence of an Fe neighbor suggests that uranyl is not directly bonded to the goethite surface in the presence of citrate. Chlorine was similarly found to provide relatively poor fits to the residual FT features. In contrast, the residual spectrum could be fit well using three carbon neighbor shells at ca 2.93, 3.1, and 4.1 Å.

A survey of the interatomic uranium–carbon distances in solid phase ring-forming complexes with oxygenated organic ligands found in the Cambridge Structure Database (26) produced the following summary: 2.8–2.9 Å for four-membered rings; 3.2–3.4 Å for five-membered rings; 3.2–3.6 Å for six-membered rings (no results available for larger rings). The 2.93-Å U–C distance is most consistent with a four-membered ring resulting from a bidentate complex with a carboxylate group, $O_2U<^{O}_{O}>C$–(R). This distance has also been reported for bidentate coordination of carbonate to uranyl and actinyl complexes (12, 10). To further constrain interpretation of this U–C distance, EXAFS spectra were collected from solutions containing uranyl–acetate complexes. EXAFS analyses of solid $UO_2(acetate)_3^-$ by Denecke *et al.* (5) yielded a uranium–carbon distance of 2.89 Å, that was interpreted in terms of a four-membered bidentate ring structure. The study by Denecke also pointed out the importance of the linear U–$C_{carboxyl}$–C_{methyl}–U multiple scattering path in the EXAFS spectra. Our fit results for aqueous $UO_2(Ac)_x^{(2-x)}$ (Table 3) are consistent with this report and with the XRD structure for solid $UO_2(acetate)_3^-$ (27). In analyzing the spectrum from $UO_2(acetate)_x^{2-x}(aq)$,[8] we considered all multiple scattering paths of up to five segments and r_{eff} up to 7 Å. The following multiple scattering paths were found to be necessary to reproduce the spectrum; linear U–$C_{carboxyl}$–C_{methyl}–$C_{carboxyl}$–U and U–$C_{carboxyl}$–C_{methyl}–U (nominally 3 and 6 paths, respectively, at $r_{eff} = 4.293$ Å for $UO_2(acetate)_3^-(aq)$) and triangular U–$C_{carboxyl}$–$O_{equatorial}$–U (nominally 12 paths at $r_{eff} = 3.28$ Å). The fits to $UO_2(acetate)_x^{2-x}(aq)$ confirm the assignment of $C_{carbonyl}$ to the EXAFS components with amplitude at 2.2–2.3 Å in the FTs. It is also significant in that a strong C signal at 4.29 Å for uranyl acetate indicates that the ring structure is rigid.

The question arises as to how one should account for the U–C distances at ca 3.1 and 4.1 Å (Table 3). These distances should be considered too short and too long, respectively, to be consistent with a monodentate U–O–C topology given the observed U–O distance of 2.39 Å and a typical value of 1.25 Å for C–O. However, the presence of C shells at these distances could be explained by larger uranyl–citrate ring structures. That contributions can be seen in such ring structures is supported by the observation of C and O atoms at 3.32 and 4.25 Å, respectively, in aqueous $PbEDTA^{2-}$ (28). In the case of citrate coordination to uranyl, it is possible to draw five-, six-, seven-, and eight-membered rings. The five- and six-membered rings require uranyl coordination to the citrate hydroxyl group. An EXAFS analysis was conducted for a sample with uranyl adsorbed on goethite in the presence of tricarballylic acid instead of citrate. Tricarballylate is similar to citrate in all aspects except it lacks a hydroxyl group at the beta position. As summarized in Table 3 (and can be seen by inspection of Fig. 2), the oxygen and carbon shell distances for the uranyl + tricarballylate + goethite sample are essentially identical to those of the uranyl + citrate + goethite samples. Therefore, five- or six-membered ring structures are not consistent with the uranyl + citrate surface species, and apparently the hydroxyl group does not play a role in the association between uranyl and citrate. This is not surprising considering the extremely high deprotonation constant for the hydroxyl group. In both citrate and tricarballylate systems the spectra for $T_{ligand} : T_U = 10 : 1$ at pH 3.5 or 5.5 also lack compelling evidence for Fe atom neighbors.

To obtain estimates of U–C distances expected in seven- and eight-membered ring uranyl–citrate complexes, gas-phase structures for citrate were calculated using the semiempirical quantum mechanical PM3 Hamiltonian and the Cache software from Oxford Molecular. The PM3 Hamiltonian was chosen because it accurately reproduces carboxylate bond lengths and angles. Cd was chosen as a surrogate for uranyl because basis sets are not readily available for uranyl and the Cd–O bond lengths are similar to those observed for $O_{equatorial}$ in the EXAFS analyses. Citrate was prevented from bonding at axial locations around the metal by placing water molecules as ligands at these locations. This model accurately reproduced the EXAFS-derived U–C distances observed in $UO_2(acetate)_x^{2-x}(aq)$. Calculations for the seven-membered ring predicted U–C distances of ca 3.2, 3.5, and 3.8 Å. In contrast, the eight-membered ring, which has a more open structure, was calculated to have U–C distances in two distinct ranges: 3.15 to 3.30 Å and 4.0 to 4.24 Å. Similar results were obtained from calculations using the AM-1 Hamiltonian for Sn(II)$(OH_2)(H_2O)_2$–citrate complexes and from simple molecular mechanics simulations of U(VI)$O_2(OH_2)(H_2O)_2$–citrate complexes. The 4.0- to 4.24-Å U–C distance is most consistent with those derived from EXAFS in the sorption samples. Based on this comparison, we tentatively conclude that the $T_{Cit} : T_U = 10 : 1$ sorption samples contain eight-membered ring structures involving uranyl and citrate. The structure derived for the eight-membered Cd(II)$(OH_2)(H_2O)_2$ complex with citrate is illustrated in Fig. 4. This structure differs from that proposed for aqueous $(UO_2)_2(citrate)_2^{2-}$, in which five- and six-membered rings were invoked (24, 25). To our knowledge,

[8] This stoichiometry is based on a predicted species distribution of 90% $UO_2(acetate)_3$ and 10% $UO_2(acetate)_2$.

the structure of aqueous UO_2(citrate)$^-$ has not been determined. It is also important to note that these basic model calculations for possible uranyl–citrate bonding structures are used primarily as a tool to aid in the interpretation of the EXAFS spectra and are not presumed to represent independent confirmation of the structures.

It is theoretically possible that uranyl bound to the goethite surface in the presence of citrate is a mixture of species. However, the excellent linear two-component fit of the spectra for samples with intermediate $T_{Cit} : T_U$ ratios would be unlikely in this case. We note that the ratio of uranyl to citrate in the surface complex would be greater than one if both bidentate and eight-membered ring structures are present simultaneously.

As mentioned earlier, adsorption of uranyl on a macroscopic scale does not follow a simple, stoichiometric relationship between the total uranyl and citrate in our experimental systems. Under the conditions used in this study, adsorption of citrate on goethite appears to be favored over the formation of a uranyl + citrate + goethite species (4). A significant fraction of citrate at low surface concentrations is not associated with uranyl. A strong association between citrate and the goethite surface is consistent with the observed high adsorption capacity of goethite for citrate ($\geq$0.8 molecule/nm^2) and the ability of citrate to reverse the net surface charge below pH 4 (29). It is plausible, and consistent with the preceding discussion, that a uranyl + citrate surface complex involves citrate acting as a bridging link. However, the number of citrate functional groups associated with goethite cannot be conclusively assigned from the present study. Overall, the relationship between uranyl adsorption and increasing surface citrate concentration could be explained by an increase in the number of carboxyl groups of adsorbed citrate that are not coordinated to the goethite surface, an increasingly negative net surface charge that promotes formation of surface species with cations (UO_2^{2+}), or simple mass action. Given the combination of bidentate and eight-membered rings structures proposed in this study, we can speculate that uranyl lies between two citrate molecules. Presumably, the complex shown in Fig. 4 would be attached to surface adsorbed citrate via a bidentate bond opposite the eight-membered ring. Since this arrangement could leave additional carboxyl groups oriented toward the solution, there could be additional capacity to complex uranyl (or other metals) and citrate in an extended polymer network.

SUMMARY

In summary, we propose the following interpretation for uranyl adsorption promoted by citrate. At pH 3.5, the dominant uranyl species is an adsorbed UO_2^{2+} + citrate complex that includes bidentate coordination with at least one carboxylate group from citrate forming a four-membered ring. Bidentate eight-membered uranyl citrate ring structures also appear to be simultaneously present, apparently as part of the same complex. The alpha hydroxyl group does not participate in coordination with uranyl. Although the EXAFS analysis cannot identify the nature of the bond with goethite, a ligand bridging structure is consistent with the aqueous sorption data based on the strength of citrate adsorption on goethite, that adsorption of anionic uranyl–citrate solution complexes would be inhibited by the negative surface charge imparted by adsorbed citrate, and the absence of evidence for an Fe neighbor in the uranyl + citrate + goethite surface species. This species exists at pH 5.5 when the concentration of adsorbed citrate is high $T_{Cit} : T_U = 10 : 1$). In the absence of citrate, uranyl adsorption occurs predominantly as an inner-sphere uranyl surface complex. This binary complex also exists as a minor species at pH 3.5 for the sample with a $T_{Cit} : T_U$ ratio of 1 : 1, suggesting that the negative surface charge induced from citrate adsorption may stabilize neighboring inner-sphere uranyl–goethite complexes. The binary complex is displaced by uranyl + citrate complex(es) as the concentration of adsorbed citrate increases. The inner-sphere uranyl–goethite surface complex found at pH 5.5, and lower $T_{Cit} : T_U$ ratios, could include an electrostatic association with citrate ions; however, an outer-sphere complex would not be expected to significantly alter the uranyl EXAFS spectra relative to the binary complex and therefore would not be observed. The possibility that multiple surface species involving uranyl and citrate are present has not been entirely excluded. Uranyl adsorption in all cases involves the formation of surface species that are distinct from solution species present under the same conditions.

ACKNOWLEDGMENTS

Special thanks and acknowledgments go to the valuable assistance of Maya Trotz with the experiments and the support of Prof. James Leckie, both from the Department of Civil and Environmental Engineering at Stanford University, Stanford, CA. We thank Steve Wasserman for his consultations regarding PCA analyses of spectra. This work was supported by DOE-BES (DE-AC03-76SF00515), DOE Office of EM under DOE Idaho Operations Office Contract DE-AC07-94ID13223, the National Institute of Environmental Health Sciences (P42 $ESO_4$940), the National Institute for Environmental Health and Safety, DOE-EMSP (54860-CA), and NIH and DOE-OBER through the SSRL Biotechnology Program.

REFERENCES

1. Davis, J. A., and Kent, D. B., *in* "Mineral–Water Interface Geochemistry, Review in Mineralogy" (M. F. Hochella and A. F. White, Eds.), p. 177. Mineralogical Society of America, Washington, DC, 1990.
2. Hue, N. V., Craddock, G. R., and Adams, F., *Soil Sci. Soc. Am. J.* **50,** 28 (1986).
3. Schwertmann, U., and Taylor, R. M., *in* "Minerals in Soil Environments" (J. B. Dixon and S. B. Weed, Eds.), p. 379. Soil Science Society of America, Madison, WI, 1989.
4. Redden, G. D., Li, J., and Leckie, J. O., *in* "Adsorption of Metals by Geomedia" (E. A. Jenne, Ed.), p. 291. Academic Press, New York, 1997.
5. Denecke, M., Reich, T., Bubner, M., Pompe, S., Heise, K., Nitsche, H., Allen, P., Bucher, J., Edelstein, N., and Shuh, D., *J. Alloys Comp.* **371,** 123 (1998).
6. Schwertmann, U., and Cornell, R. M., "Iron Oxides in the Laboratory." VCH, New York, 1991.
7. Papelis, S., Hayes, K. F., and Leckie, J. O., "HYDRAQL: A Program for the Computation of Chemical Equilibrium Composition of Aqueous Batch Systems Including Surface-Complexation Modeling of Ion Adsorption at the Oxide/Solution Interface." Environmental Engineering and Science, Dept. of Civil Engineering; Stanford, CA, 1988.
8. Rajan, K. S., and Martell, A. E., *Inorg. Chem.* **4,** 462 (1964).
9. Grenthe, I., Fuger, J., Konigs, R. J. M., Lemire, R. J., Muller, A. B., Nguyen-Trung, C., and Wanner, H., "Chemical Thermodynamics of Uranium," Vol. 1. Elsevier, Holland, 1992.
10. Clark, D. L., Hobart, D. E., and Neu, M. P., *Chem. Rev.* **95,** 25 (1995).
11. Smith, R. M., and Martell, A. E., "NIST Critical Stability Constants of Metal Complexes Database, V4.0." U.S. Dept. of Commerce: Gaithersburg, MD, 1997.
12. Bargar, J. R., Reitmeyer, R., Lenhart, J. J., and Davis, J. A., *Geochim. Cosmochim. Acta* **64,** 2737 (2000).
13. George, G. N., "EXAFSPAK." Stanford Synchrotron Radiation Laboratory, Stanford, CA, 1993.
14. Fuller, C., Bargar, J. R., Davis, J. A., and Piana, M., *Environ. Sci. Technol.*, submitted for publication.
15. Ressler, T., "WinXAS." 2001: Department of Inorganic Chemistry, Faradayweg 4-6, D-14195 Berlin, Germany.
16. Wasserman, S. R., *J. Phys.* **7**(C2), 203 (1997).
17. Ressler, T., Wong, J., Roos, J., and Smith, I. L., *Environ. Sci. Technol.* **34**(6), 950 (2001).
18. De Leon, J. M., Rehr, J. J., and Zabinshy, S. I., *Phys. Rev. B* **44**(9), 4146 (1991).
19. Rehr, J. J., De Leon, J. M., Zabinsky, S. I., and Albers, R. C., *J. Am. Chem. Soc.* **113**(14), 5135 (1991).

20. Bargar, J. R., Brown, Jr., G. E., and Parks, G. A., *Geochim. Cosmochim. Acta* **61**(13), 2617 (1997).
21. Hudson, E. A., Allen, P. G., Terminello, L. J., Denecke, M. A., and Reich, T., *Phys. Rev. B* **54**(1), 156 (1996).
22. Bargar, J. R., Reitmeyer, R., and Davis, J. A., *Environ. Sci. Technol.* **33,** 2481 (1991).
23. Borkowski, M., Lis, S., and Choppin, G. R., *Radiochim. Acta* **74,** 117 (1996).
24. Allen, P. G., Shuh, D. K., Bucher, J. J., Edelstein, N. M., Reich, T., Denecke, M. A., and Nitsche, H., *Inorg. Chem.* **35,** 784 (1996).
25. Nunes, M. T., and Gil, V. M. S., *Inorg. Chem. Acta* **129,** 283 (1987).
26. Allen, F. H., and Kennard, O., *Chem. Des. Autom. News* **8,** 131 (1993).
27. Templeton, D. H., Zalkin, A., Ruben, H., and Templeton, L. K., *Acta Crystallogr. C* **41**(Oct), 1439 (1985).
28. Bargar, J. R., Persson, P., and Brown, G. E., *Geochim. Cosmochim. Acta* **63**(19–20), 2957 (1999).
29. Redden, G. D., Persson, P., and Bencheikh-Latmani, R., *in* "American Chemical Society, Spring 1997." American Chemical Society, San Francisco, CA, 1997.

George Redden*,[1]
John Bargar†
Rizlan Bencheikh-Latmani‡,[2]

**Idaho National Engineering and Environmental Laboratory*
PO Box 1625, MS 2208
Idaho Falls, Idaho 83415
†Stanford Synchrotron Radiation Laboratory
Stanford, California 94305
‡Department of Civil and Environmental Engineering
Stanford University, Stanford, California 94305

Received October 23, 2000; accepted September 20, 2001

[1] To whom correspondence should be addressed. Fax: (208) 526-8541. E-mail: reddgd@inel.gov.
[2] Current address: Marine Biology Division, Scripps Institution of Oceanography, La Jolla, CA 92093.